Microcavity OLED using Ag electrodes

Huajun Peng, Xiuling Zhu, Jiaxin Sun, Xiaoming Yu, Man Wong and Hoi-Sing Kwok

Center for Display Research, Department of Electrical and Electronic Engineering
Hong Kong University of Science and Technology, Clear Water Bay, Hong Kong, China

ABSTRACT

We examine various OLED configurations using semitransparent Ag as the electrode. With thin Ag as the anode and Al as the cathode, a bottom emitting microcavity can be formed. With thin Ag as the cathode and thick Ag as the anode, a top-emitting microcavity can be formed. In both cases, the OLED coupling efficiency can be improved greatly with enhanced emission. Using triplet emitters, a power efficiency of 80 lm/W and a current efficiency of 80 cd/A can be achieved in a bottom emitting device.

Keywords: OLED, microcavity, metal electrodes, silver.

1. INTRODUCTION

Efficient organic light emitting diode (OLED) is now routinely fabricated. The external quantum efficiency of an OLED is a product of (1) the internal quantum efficiency, (2) the light coupling efficiency of the device. The internal quantum efficiency can approach 100% with the use of triplet emitters [1,2]. However the coupling efficiency is still in dire need of improvement.

The coupling efficiency is given approximately by

$$\eta_{coupling} = \frac{1}{\varepsilon n^2} \tag{1}$$

where ε is a factor dependent on the emission geometry and n is the refractive index of the OLED material. For most OLED, this factor is about 22%. Thus most of the light from the OLED is trapped inside the OLED which acts as a waveguide. There are also light trapped in the glass substrate as well for bottom emitting devices.

Several methods have been reported in the literature to improve the coupling efficiency of OLEDs, such as using microcavity, microlens array, low index substrate, nanopatterned photonic crystals etc [3-7]. They all have their merits and drawbacks. Improvement is typically in the range of 1.5-2.0. The microcavity structure has been mostly studied because of it does not involve too much extra effort in fabricating the device. A microcavity OLED usually consists of an asymmetrical structure with the organic layers sandwiched between a highly reflective metallic mirror and an ITO coated distributed Bragg reflector (DBR) [3,4]. However, the multilayer dielectric thin film structure of the DBR makes the fabrication process complicated. As well, the thickness of the DBR makes the angular color shift intolerably large. The alternative approach of utilizing a single semitransparent metal layer as the reflector is more desirable.

Semitransparent metal reflectors with low absorption have been used in top emitting OLEDs as the top cathode. These top emitting devices also show higher coupling efficiency than the equivalent bottom-emitting device due to a strong microcavity effect [8-11]. In this work, we show that thin semitransparent Ag can act as a good electrode for OLEDs. It can be used as a cathode as well as an anode. As a cathode, it can be used to make a top emitting device. With semitransparent Ag as the anode, a good bottom emitting device can be consgtructed. In both cases, microcavity effect is strong. Such microcavity effect can be used to enhance the coupling efficiency of the OLED.

There are two issues with using a metallic electrodes: (1) the hole or electron injection efficiency has to be good, and (2) the microcavity effect has to be optimized. With semitransparent Ag, we demonstrate a new method of reducing the barrier height for efficient current injection. Using a phosphorescent material, $Ir(ppy)_3$, the Ag anode bottom emitting

device exhibits a maximum efficiency of 81± 8cd/A and a power efficiency of 79± 8 lm/W. This is much better than the results of 46± 4.5 cd/A and 39 ± 4 lm/W for a similar ITO anode device. This improvement is mainly due to the higher coupling efficiency and enhanced hole injection in the Ag anode devices. Similarly efficient top emitting OLED can also be fabricated.

2. SILVER ELECTRODE

There are many possible choices for the metal electrode. A good choice should take into account of the metal work function and its transparency. Fig. 1 shows the absorption of several metals in the visible spectrum. It can be seen that silver is the best choice in terms of low loss. So the only remaining question is whether Ag can be used as an electrode for good electron or hole injection. We have recently invented a process of surface treatment of the Ag electrode. After this plasma treatment, the hole injection efficiency of Ag is greatly improved. Fig. 2 shows the hole injection efficiency of the Ag anode before and after the plasma treatment. It can be seen that there is indeed a great improvement in the current injection capability for Ag.

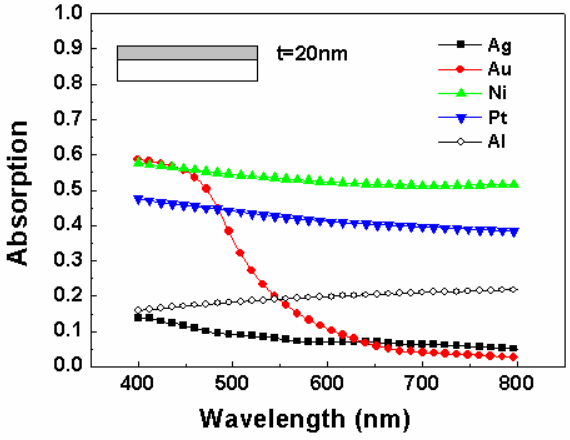

Figure 1. Absorption of 20nm thick metal films.

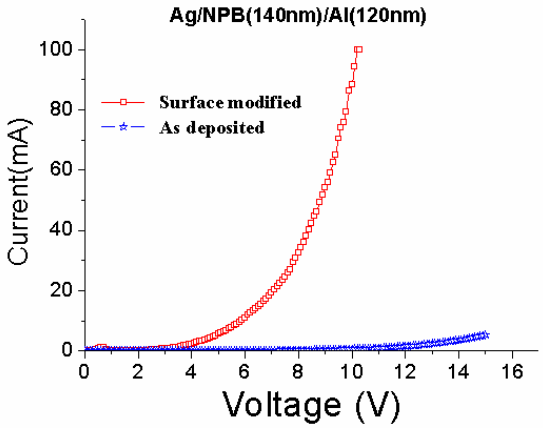

Figure 2. Hole injection efficiency of native and modified Ag.

3. MICROCAVITY EFFECT

We model both the ITO and Ag OLEDs in order to calculate how much power is emitted into different optical modes. The optics of a planar structure OLED is analyzed by a classical model based on the equivalence between the emission of a photon due to an exciton's radiative decay and the radiation of a classical electrical dipole [12-14]. In this model the power generated $\overline{P}$ by a dipole source can be expressed as an integral over the in-plane wavevector $k_{//}$,

$$\overline{P} = \int_0^\infty K(k_{//})dk_{//} \qquad (2)$$

where the quantity $K(k_{//})$ is defined as the $k_{//}$-space power spectrum. The distribution of the radiation power into different plane-wave modes can be identified with different regions of this $k_{//}$ integration. The calculated power can be used as a benchmark for optimizing device layer thickness for a high coupling efficiency. In addition, comparing the fraction of the light in each mode type lends insight into how the Ag anode device can provide improvement in coupling efficiency.

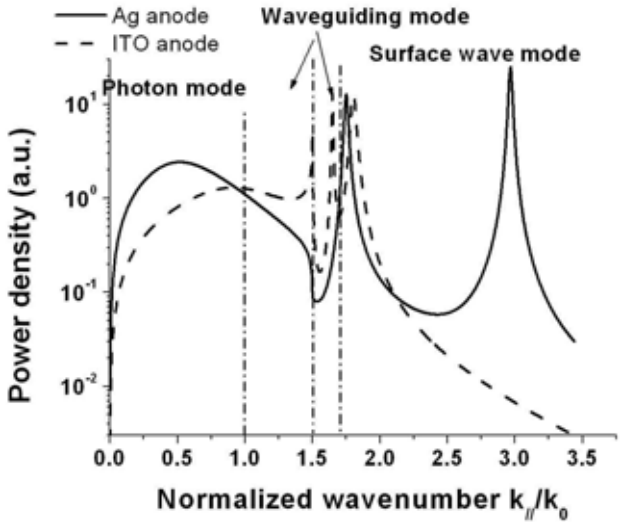

Figure 3. Calculated $k_{//}$-space power spectra.

Fig. 3 shows the results for the cases of an oscillating dipole embedded in the ITO anode device and Ag anode device, where the dipole is located at the emission zone with random orientation. The power spectra can be divided into four regions according to the $k_{//}$ value. Region I ($0 \le k_{//} \le k_0$) [15], corresponds to the photon emission mode, i.e. it gives the portion of the total light that can be extracted from the device surface as useful radiation. Region II ($k_0 \le k_{//} \le 1.5k_0$) and III ($1.5k_0 \le k_{//} \le 1.7k_0$) correspond to waveguiding modes in the glass substrate and the organic/ITO layers, respectively. The narrow peaks in region IV ($1.7k_0 \le k_{//}$) are the surface wave modes, corresponding to evanescent surface waves propagating along the metallic electrode surface [14]. Only the photon mode represents light coupled out while the other modes represent losses. It can be seen that for the Ag anode structure, the power density of the photon mode is much higher than that of convention ITO anode structure. At the same time, the power of waveguide modes in both glass and organic layers are significantly suppressed. This change of the power dissipation clearly indicates the enhanced light extraction from the Ag anode device. Comparing the integrated power in the photon modes of two devices, we expect an enhancement factor of 1.7 for the Ag anode device.

The emission characteristics of microcavity OLEDs can be accurately described by a model based on dipole radiation in a multilayer thin film structure [17,18]. In the normal direction, EL intensity is described as

$$I(\lambda) \propto \frac{\left|1+\sqrt{R_1}\,exp\left[j\left(4\pi n_0 z / \lambda + \phi_1\right)\right]\right|^2}{\left|1-\sqrt{R_1 R_2}\,exp\left[j\left(4\pi n_0 d / \lambda + \phi_1 + \phi_2\right)\right]\right|^2} T_2(\lambda) \qquad (3)$$

where R_2 and T_2 are the respective reflectance and transmittance of the top semitransparent cathode; R_1 is the reflectance of the bottom opaque anode; ϕ_1 and ϕ_2 are the respective phase change of reflectance at two interfaces, and n_0 is the refractive index of the medium between the electrodes; z is the distance between dipole and Ag anode; d is the cavity length; and λ is the emission wavelength in vacuum. Based on eq. (3), with increase of the Ag cathode thickness, the transmittance T_2 decreases while the reflectance R_2 increases, which leads mathematically to a maximum value of the output intensity at the Ag cathode thickness about 24 nm. The calculation result was scaled to give the best fit to the experiment and the agreement was excellent. These results indicate that the thickness of the semitransparent top layer plays an important role in determining the device efficiency.

4. BOTTOM EMITTING OLED

Two bottom emitting OLEDs with different anodes were then fabricated to verify the predictions. For the ITO anode

device, 750 Å thick indium tin oxide (ITO) film was deposited by RF sputtering on glass substrates. For the Ag anode device, a 250 Å thick Ag film was deposited by thermal evaporation onto glass substrates. In both devices, we used 4,4'-bis(1-napthyl-N-phenyl-amino)- biphenyl (NPB) as the hole transport layer, 4,4'-*N*,*N*'-dicarbazole-biphenyl (CBP) doped with fac tris (2-phenylpyridine) iridium ($Ir(ppy)_3$) as the emitter layer, 1,3,5-Tris (N-phenylbenzimidazol-2-yl)benzene (TPBi) as the electron injection layer, and LiF/Al as the composite cathode. The structure of the ITO anode device consists of ITO(75nm)/NPB(70nm)/CBP:$Ir(ppy)_3$(8 wt %, 25nm)/TPBi(40nm)/LiF(1nm)/Al(110nm). The structure of the Ag anode device consists of Ag (25nm)/NPB(52nm)/CBP:$Ir(ppy)_3$(8 wt%, 20nm)/TPBi(40nm)/LiF(1nm)/Al (110nm). The layer thicknesses of both devices have been optimized based on a model calculation. For the Ag anode device, both the anode and organic layer thicknesses were carefully tuned to strike a balance the coupling efficiency enhancement and emission color variation. All the materials in the devices, including the semitransparent Ag anode were deposited by thermal evaporation in a multi-chamber vacuum system without breaking the vacuum. The base pressure of the system was $<1x10^{-4}$. In order to avoid cross contamination, the organic materials and the metals were deposited in two independent chambers separated by a gate valve.

The Current density(J) - Voltage (V) - Luminance (L) characteristics of both devices were measured using an HP4145B semiconductor parameter analyzer and a large diameter (2.5cm) photodiode. The external quantum efficiencies of the devices were measured directly by placing the device about 2 mm over the photodiode. The spectral characterization and the luminance calibration of the photodiode were carefully performed with a PhotoResearch PR650 spectroradiometer. In the measurement, a Lambertian distribution is assumed for the ITO anode device while the non-lambertian emission profile has to be taken account for the Ag anode device. Its angular dependence has to be measured in order to calculate the total emission.

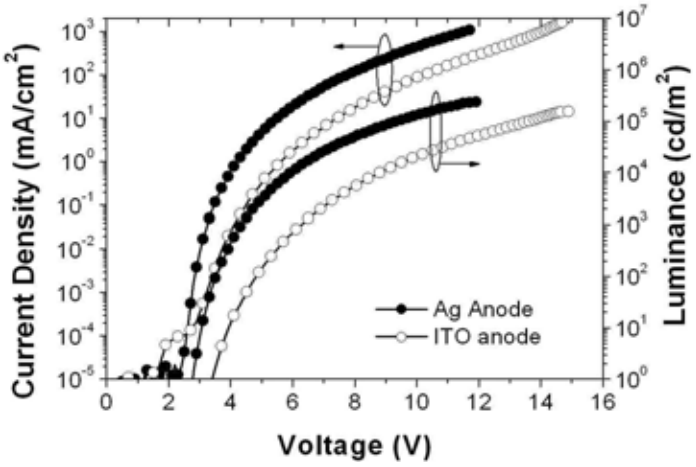

Figure 4. Electrooptic properties of bottom emitting OLEDs.

Fig. 4 compares the current density (J) - luminance (L) – voltage (V) of the two devices. The Ag anode device shows a performance superior to that of the ITO anode device in both the L-V and J-V curves. For instance, the turn-on voltages for light emission of 1 cd/m^2 is about 2.7 V for Ag anode device and 3.3 V for the ITO anode device. The voltages to obtain a luminance of 1000 cd/m^2 for the two devices are 4.6 and 6.2 V. And the driving voltages at a current density of 100 mA/cm^2 for devices with the Ag and ITO anode are 7.8 and 10.3 V, respectively.

Having a reflecting anode and cathode, the Ag anode device is expected to exhibit strong microcavity effects on both the spectral and spatial distribution of the emission. Fig. 5(a) shows the EL spectra measured under a current of 2 mA/cm^2 at viewing angles from 0° to 60° for the Ag anode device. It can be seen that when the viewing angle increases, the emission peak shifts from 536nm to 516 nm. Although there is some angle dependency in the spectrum, the corresponding 1931 CIE color coordinates are still much close to the NTSC standard green, as shown in the inset of Fig. 4(a). The simulated EL spectra with relative intensities are given in Fig. 5(b). It can be seen that the measured spectra and relative intensities agree quite will with the calculated ones, confirming the accuracy of the simulation.

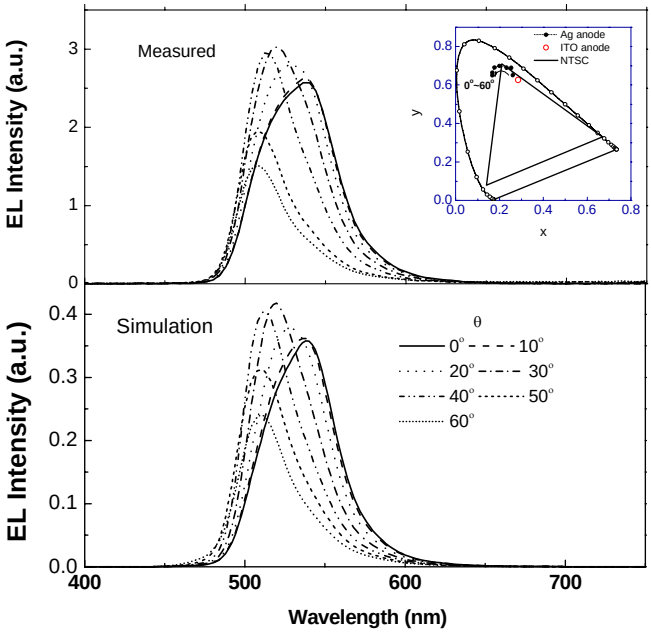

Figure 5. Angular dependence of emission spectra.

Fig. 6 shows the power efficiency (η_P) and the current efficiency (η_J) of both devices. The maximum η_J and η_P of the Ag anode device are 81±8 cd/A and 79±8 lm/W, respectively, compared with those of 46±5 cd/A and 39±4 lm/W for the ITO anode device. At the luminance of 1000 cd/m^2, the Ag anode device still demonstrates a high power efficiency of 47±4.7 lm/W, compared with that of 21±2 lm/W for the ITO anode device.

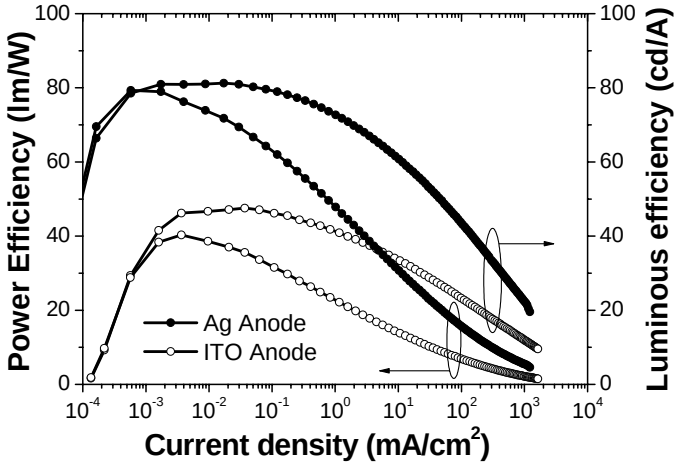

Figure 6. Efficiencies of the microcavity OLED.

The superior performance of the Ag anode device can be attributed to the enhanced hole injection ability and the enhanced coupling efficiency in the microcavity structure. It is noticed that the enhancement factor of the power efficiency (η_P) is larger than that of the current efficiency (η_J). The reason is that the enhanced hole injection causes the lower driving voltage of the Ag anode device which consumes less electrical power to obtain the identical current density.

The mechanism for the hole injection enhancement of Ag anode has been discussed in our previous report [17]. The improvement of η_J is mostly attributed to the enhanced coupling efficiency. Because the current efficiency is dependent on the photopic response of eyes, a better indicator of the efficiency of the device is the external quantum efficiency, η_{EQE}. An external quantum efficiency of 12.3±1% at 10uA/cm^2 was achieved for the ITO anode device, similar to the recently reported results by Liao et al [18].

5. TOP EMITTING OLED

Top emitting OLED (TOLED) are important in increasing the aperture ratio of active matrix devices. For the cathodes of TOLEDs, semi-transparent metal films or compound such as (Mg:Ag) [19], Ca/Mg [20,21], Ca/Ag [22] , or LiF/Al/Ag [23] have been adopted. The TOLEDs using semitransparent metallic cathode shows modified emission properties due to the strong microcavity effect. In this section, we report on TOLEDs that use thick Ag as the reflective anode and semitransparent Ag as the cathode. With proper surface treatment on the Ag anode and optimization of the cathode Ag thickness, the resulting TOLEDs demonstrate superior optical and electrical characteristics over the conventional bottom emitting OLEDs using ITO anode.

To fabricate the devices, a patterned 80nm thick Ag film was first deposited on glass substrate through a shadow mask, and then pretreated under CF_4 plasma [24]. After surface pretreatment, the sample was loaded into an evaporation chamber at a base pressure of 7x10^{-7} Torr for organic film deposition. The organic multilayer structure sequentially consists of alpha-napthylphenylbiphenyl diamine (NPB, 56nm) as hole transport layer, tris-8-hydroxyquinoline aluminum (Alq_3, 25nm) doped with 1 wt% 10-(2-benzothiazolyl)-1,1, 7,7-tetramethyl-2,3,6,7- tetrahydro-1H,5H,11H -[l]benzo-pyrano[6,7,8-ij]quinolizin-11-one (C545T) as emitting layer, and undoped Alq_3 (30nm) as electron transport layer. The sample was then transferred to another chamber without breaking vacuum for cathode deposition. To achieve both desired optical transmission and effective electron injection, we applied multiple functional layers consisting of LiF(0.8 nm)/Al(2 nm)/Ag (x nm). The 2nm thick Al film on LiF on Alq_3 is sufficient to enhance the electron injection with a negligible effect on the optical properties of the cathode [24]. We tune the top Ag thickness from 12 nm to 50nm to compare the devices performance. The structure is shown in the inset of Fig. 7. For comparison, bottom emitting OLEDs with the same layer structures except the anode formed by 75nm thick ITO coated on glass substrate and cathode by LiF(0.8nm)/Al (120nm) were fabricated. Another control device using as deposited Ag without CF_4 pretreatment was also fabricated.

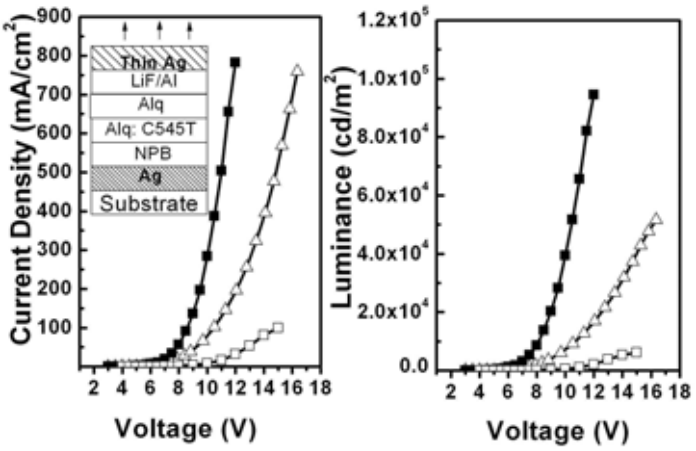

Figure 7. Electrooptic properties of TOLEDs.

Figure 7 compares the current density (J) - normal direction luminance (L) – voltage (V) characteristics of the reference OLED and the TOLEDs using 20nm Ag cathode. The voltage drop on the electrode lines were subtracted for comparison. The TOLED using as-deposited Ag anode shows rather poor performances. On the other hand, the TOLED using surface modified Ag anode demonstrates performances superior to that of the bottom emitting device, in both J-V

and L-V curves. For instance, the TOLED has a turn-on voltage as low as 2.65 V, compared with 2.85 V for the OLED to obtain a brightness of 1 cd/m^2. And the voltages to obtain a luminance of 1000 cd/m^2 for the two devices are 6.1 and 7.0 V, respectively. With voltage increase, both the current density and luminance of the Ag anode TOLED increase faster than those of the OLED, reaching the maximum values of 783 mA/cm^2 and 94,400 cd/m^2 at 12 V, respectively. In contrast, the control OLED reaches its maximum current density of 760 mA/cm^2 and luminance of 51,600 cd/m^2 at 16.5 V. The superior JV performance is attributed to the enhanced hole injection of the Ag anode with CF_4 plasma pretreatment. It is proposed that hole injection barrier is effectively reduced by means of formation of a localized interface dipole layer with deposition of an ultrathin CFx layer on the Ag anode surface after CF_4 plasma treatment [25]. The difference between the LV curves of TOLED and bottom emitting OLED is bigger than that between the JV curves. This discrepancy infers the tailored emission performance of TOLEDs by an optical microcavity. A TOLED with an optimized structure design would provide a higher current efficiency then bottom emitting devices. For brevity, the TOLEDs mentioned in the following discussion refer to the devices using surface pretreated Ag as anode.

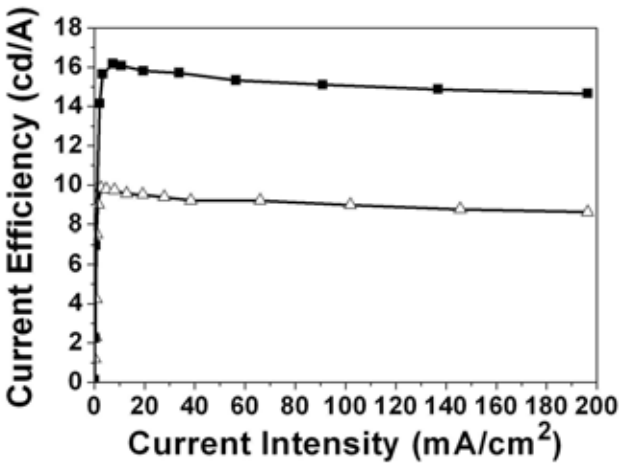

Figure 8. Current efficencies of TOLEDs.

Fig. 8 shows the current efficiency η_J as function of current density of the reference OLED and the TOLEDs using 20nm Ag cathode. At 10 mA/cm ^{2}, the TOLED demonstrate a high efficiency of 16.1 cd/A, 65% higher than that of 9.6 cd/A for the OLED. Sharing the same organic/metal interface states, all TOLEDs with different Ag cathode thickness demonstrate the identical JV curves with measurement uncertainty (not shown). On the other hand, the efficiency changes significantly by tuning the Ag cap thickness. The experimental data show a η_J of 13.1 cd/A at an Ag thickness of 12nm. With Ag thickness increase, efficiency rise 25% to 16.1 cd/A; and then falls to 14.3 cd/A at an Ag thickness of 30nm, 10.1 cd/A at an Ag thickness of 40nm. The absorption of the Ag in the range differs actually by less than 2%, according to the calculation results. Therefore, the difference in efficiency is attributed to the variation of the transmission and reflection of the Ag films.

6. CONCLUSIONS

In summary, it can be seen that Ag can be used as both a cathode and an anode in microcavity OLED. Using optimal thicknesses, the microcavity effect can be used to increase the coupling efficiency of the OLED. Results reported here indicate that high efficiency can be achieved. This process is compatible with conventional OLED fabrication and does not involve new materials. It is believed that it can be used in both passive as well as active matrix devices.

ACKNOWLEDGMENTS

This research was supported by the Hong Kong SAR government Innovations and Technology Fund.

REFERENCES

[1] C. Adachi, M. A. Baldo, M. E. Thompson, S. R. Forrest, J. Appl. Phys.,**90**, 5048 (2001).
[2] M. Ikai, S. Tokito, Y. Sakamoto, T. Suzuki, and Y. Taga, Appl. Phys. Lett. **79**, 156 (2001).
[3] R.H. Jordan, L. J. Rothberg, A. Dodabalapur, and R. E. Slusher, Appl. Phys. Lett., **69**, 1997 (1996).
[4] H. J. Peng, M. Wong, and H. S. Kwok, SID03 Digest, p516 (2003).
[5] S. Möller and S. R. Forrest, J. Appl. Phys. **91**, 3324 (2002).
[6] T. Tsutsui, M. Yahiro, H. Yokogawa, K. Kawano, M. Yokoyama, Adv. Mater., **13**, 1149 (2001).
[7] C. W. Chen, P. Y. Hsieh, H. H. Chiang, C. L. Lin, H. M. Wu, and C. C. Wu, Appl. Phys. Lett. 83, 5127 (2003)
[8] Y.J. Lee, S. H. Kim, J. Huh, G. H. Kim, Y. H. Lee, S. H. Cho, Y. C. Kim, and Y. R. Do, Appl. Phys. Lett. **82**, 3779 (2003).
[9] M. H. Lu and J. C. Sturm, J. Appl. Phys. **92**. 595 (2002).
[10] H. J. Peng, M. Wong and H. S. Kwok, Soc. for Info. Display Symp. Digest, vol. 34, p.516, (2003).
[11] H. Riel, S. Karg, T. Beierlein, B. Ruhstaller, and W. Riess, Appl. Phys. Lett. **82**, 466 (2003).
[12] W. Lukosz, Phys. Rev. B., **22**, 3030 (1980).
[13] K. Neyts, P. de Visschere, D. K. Fork, and G. B. Anderson, J. Opt. Soc. Am. B, **17**, 114 (2000).
[14] G. W. Ford and W. H. Weber, Phys. Rep. **113**, 195 (1984).
[15] The wavenumber k_o is determined by $k_o = 2\pi / \lambda_o$, λ_0 is set to be 520 nm, a little larger than the peak wavelength of photoluminescence spectrum of emitting material which is 512nm for $Ir(ppy)_3$.
[16] H. B. Michaelson, IBM J. Res. Dev. **22**, 72 (1978).
[17] H. J. Peng, M. Wong, and H. S. Kwok, submitted to Appl.. Phys. Lett.
[18] L. S. Liao, K. P. Klubek, and C. W. Tang, Appl. Phys. Lett. **84**, 167 (2003).
[19] G. Gu, V. Bulovic, P. E. Burrows, S. R. Forrest, and M. E. Thompson, Appl. Phys. Lett., 68, 2606 (1996)
[20] H. Riel, S. Karg, T. Beierlein, B. Ruhstaller, and W. Riess, Appl. Phys. Lett. 82, 466(2003)
[21] H. Riel, S. Karg, T. Beierlein, B. Ruhstaller, W. Riess, and K. Neyts, J. Appl. Phys. 94, 5290 (2003)
[22] R. B. Pode, C. J. Lee, D. G. Moon, and J. I. Han, Appl. Phys. Lett. 84, 4614 (2004)
[23] L. S. Hung, C. W. Tang, M. G. Mason, P. Raychaudhuri, and J. Madathil, Appl. Phys. Lett., 78,544(2001)
[24] K. Neyts, P. de Visschere, D. K. Fork, and G. B. Anderson, J. Opt. Soc. Am. B, 17, 114(2000)
[25] C. F. Qiu, H. J. Peng, H. Y. Chen, Z. L. Xie, M. Wong and H. S. Kwok, IEEE Transactions on Electron Devices, **51**, 1208(2004)